

# Om and Statefinder Diagnostics of Anisotropic $f(R, \mathcal{L}_m)$ Gravity

**Prof. Dr. Dnyaneshwar D. Pawar**

Professor and Director

School of Mathematical Sceiences,

Swami Ramanand Teerth Marathwada University, Nanded, MH-India

**CosmoFondue, 12, Jun 2025**

# $f(R, \mathcal{L}_m)$ Theory of Gravity

- The action for  $f(R, \mathcal{L}_m)$  gravity, proposed by Harko and Lobo, is:

$$S = \int f(R, \mathcal{L}_m) \sqrt{-g} d^4x, \quad (1)$$

where  $f$  is a general function of the Ricci scalar  $R$  and the matter Lagrangian  $\mathcal{L}_m$ .

- The Ricci scalar is defined as:

$$R = g^{ij} R_{ij}. \quad (2)$$

- The Ricci tensor is given by:

$$R_{ij} = \partial_k \Gamma_{ij}^k - \partial_j \Gamma_{ki}^k + \Gamma_{ij}^\lambda \Gamma_{\lambda k}^k - \Gamma_{j\lambda}^k \Gamma_{ki}^\lambda. \quad (3)$$

## $f(R, \mathcal{L}_m)$ Theory of Gravity

- Varying the action with respect to the metric yields the field equations:

$$f_R R_{ij} - \frac{1}{2}(f - f_{\mathcal{L}_m} \mathcal{L}_m) g_{ij} + (g_{ij} \square - \nabla_i \nabla_j) f_R = \frac{1}{2} f_{\mathcal{L}_m} T_{ij}. \quad (4)$$

- Here, the partial derivatives of  $f$  are:

$$\begin{aligned} f_R &= \frac{\partial f(R, \mathcal{L}_m)}{\partial R}, \\ f_{\mathcal{L}_m} &= \frac{\partial f(R, \mathcal{L}_m)}{\partial \mathcal{L}_m}, \\ \square &= \nabla_i \nabla^i. \end{aligned}$$

- The energy-momentum tensor is defined by:

$$T_{ij} = g_{ij} \mathcal{L}_m - 2 \frac{\partial \mathcal{L}_m}{\partial g^{ij}}. \quad (5)$$

## $f(R, \mathcal{L}_m)$ Theory of Gravity

- The covariant divergence of the energy-momentum tensor is given by:

$$\nabla^i T_{ij} = 2\nabla^i \ln(f_{\mathcal{L}_m}) \frac{\partial \mathcal{L}_m}{\partial g^{ij}}. \quad (6)$$

- Contracting the field equations leads to the trace relation:

$$Rf_R + 3\Box f_R - (f - f_{\mathcal{L}_m}\mathcal{L}_m) = \frac{1}{2}f_{\mathcal{L}_m}T, \quad (7)$$

where  $T = g^{ij}T_{ij}$  is the trace of the energy-momentum tensor.

- The d'Alembertian operator  $\Box$  acting on a scalar  $F$  is defined as:

$$\Box F = \frac{1}{\sqrt{-g}} \partial_i (\sqrt{-g} g^{ij} \partial_j F).$$

## Equation of Motion in $f(R, \mathcal{L}_m)$ Gravity

- Anisotropic cosmological models introduce extra degrees of freedom and richer dynamics compared to isotropic ones like FLRW, though they are more challenging to analyze.
- We consider a homogeneous and anisotropic LRS Bianchi Type-I spacetime:

$$ds^2 = -dt^2 + A^2(t)dx^2 + B^2(t)(dy^2 + dz^2), \quad (8)$$

where  $A(t)$  and  $B(t)$  are scale factors in cosmic time.

- For  $A(t) = B(t)$ , this reduces to the standard FLRW metric.
- The Ricci scalar for this metric is:

$$R = -2 \left[ \frac{\ddot{A}}{A} + 2\frac{\ddot{B}}{B} + 2\frac{\dot{A}\dot{B}}{AB} + \frac{\dot{B}^2}{B^2} \right]. \quad (9)$$

- Assuming a perfect fluid distribution, the energy-momentum tensor is:

$$T_{ij} = (p + \rho)u_i u_j + p g_{ij}, \quad (10)$$

where  $\rho$  is energy density,  $p$  is pressure, and  $u^i = (1, 0, 0, 0)$  is the comoving four-velocity.

# Equation of Motion in $f(R, \mathcal{L}_m)$ Gravity

- The modified Friedmann-like field equations in  $f(R, \mathcal{L}_m)$  gravity for the Bianchi Type-I metric are given as:

$$-\left(\frac{\ddot{A}}{A} + 2\frac{\dot{A}\dot{B}}{AB}\right) f_R - \frac{1}{2}(f - f_{\mathcal{L}_m}\mathcal{L}_m) - 2\frac{\dot{B}}{B}\dot{f}_R - \ddot{f}_R = \frac{1}{2}f_{\mathcal{L}_m}p, \quad (11)$$

$$-\left(\frac{\ddot{B}}{B} + \frac{\dot{B}^2}{B^2} + \frac{\dot{A}\dot{B}}{AB}\right) f_R - \frac{1}{2}(f - f_{\mathcal{L}_m}\mathcal{L}_m) - \left(\frac{\dot{A}}{A} + \frac{\dot{B}}{B}\right) \dot{f}_R - \ddot{f}_R = \frac{1}{2}f_{\mathcal{L}_m}p, \quad (12)$$

$$-\left(\frac{\ddot{A}}{A} + 2\frac{\ddot{B}}{B}\right) f_R - \frac{1}{2}(f - f_{\mathcal{L}_m}\mathcal{L}_m) - \left(\frac{\dot{A}}{A} + 2\frac{\dot{B}}{B}\right) \dot{f}_R = \frac{1}{2}f_{\mathcal{L}_m}\rho. \quad (13)$$

- Here,  $f_R = \partial f / \partial R$ ,  $f_{\mathcal{L}_m} = \partial f / \partial \mathcal{L}_m$ , and dots denote derivatives with respect to cosmic time  $t$ .

# Cosmological Solutions for $f(R, \mathcal{L}_m)$ Gravity

- We consider a specific form of the function:

$$f(R, \mathcal{L}_m) = \frac{R}{2} + \mathcal{L}_m^\xi + \zeta, \quad (14)$$

where  $\xi$  and  $\zeta$  are constants. GR is recovered when  $\xi = 1$  and  $\zeta = 0$ .

- Assuming a dust-like Universe ( $\mathcal{L}_m = \rho$ ), the modified field equations become:

$$2\frac{\ddot{B}}{B} + \frac{\dot{B}^2}{B^2} - \zeta - (1 - \xi)\rho^\xi = \xi\rho^{\xi-1}p, \quad (15)$$

$$\frac{\ddot{A}}{A} + \frac{\ddot{B}}{B} + \frac{\dot{A}\dot{B}}{AB} - \zeta - (1 - \xi)\rho^\xi = \xi\rho^{\xi-1}p, \quad (16)$$

$$\frac{\dot{B}^2}{B^2} + 2\frac{\dot{A}\dot{B}}{AB} - \zeta = (1 - 2\xi)\rho^\xi. \quad (17)$$

# Cosmological Solutions for $f(R, \mathcal{L}_m)$ Gravity

- To solve the system, we use a deceleration parameter approach as in Tiwari et al. **[16]**, where:

$$q = \frac{-a\ddot{a}}{\dot{a}^2}, \quad \text{with} \quad q(t) = \alpha - \frac{\beta}{H}. \quad (18)$$

- The average scale factor is:

$$a = (AB^2)^{1/3}, \quad (19)$$

which solves to:

$$a = \left( \frac{\alpha + 1}{\beta c} e^{\beta t} + c_1 \right)^{\frac{1}{\alpha+1}}. \quad (20)$$



# Cosmological Solutions for $f(R, \mathcal{L}_m)$ Gravity

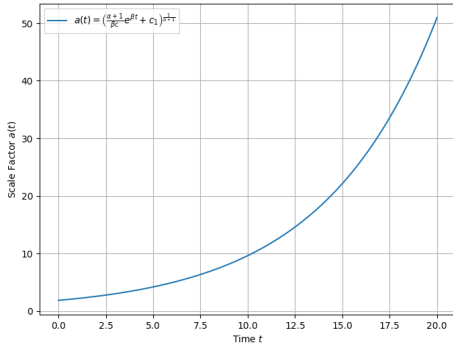


figure Evolution of the scale factor  $a(t)$  with cosmic time  $t$ .

- The evolution of the scale factor  $a(t)$  provides insight into the Universe's expansion dynamics.
- Initially, the Universe exhibits slower expansion, corresponding to a decelerated phase dominated by matter.
- As time progresses, the scale factor increases rapidly, signaling a transition to an accelerated expansion phase.
- This late-time acceleration aligns with current cosmological observations of dark energy-driven expansion.

# Cosmological Solutions for $f(R, \mathcal{L}_m)$ Gravity

- Using the power-law relation, the metric functions become:

$$B(t) = \left( \frac{\alpha + 1}{\beta c} e^{\beta t} + c_1 \right)^{\frac{3}{(\alpha+1)(2+n)}}, \quad (21)$$

$$A(t) = \left( \frac{\alpha + 1}{\beta c} e^{\beta t} + c_1 \right)^{\frac{3n}{(\alpha+1)(2+n)}}. \quad (22)$$

- The line element now simplifies to:

$$ds^2 = -dt^2 + A^2(t)dx^2 + B^2(t)(dy^2 + dz^2), \quad (23)$$

showing anisotropic expansion with time-dependent scale factors.

# Hubble Parameter

- Redshift  $z$  is related to the scale factor via:

$$a = \frac{1}{1+z}, \quad \text{with } a = 1 \text{ at } z = 0.$$

- For the model  $f(R, \mathcal{L}_m) = \frac{R}{2} + \mathcal{L}_m^\xi + \zeta$ , the Hubble parameter becomes:

$$H(z) = \frac{\beta}{\alpha + 1} [1 - c_1(1+z)^{\alpha+1}],$$

$$H_0 = \frac{\beta}{\alpha + 1} (1 - c_1).$$

- Model predictions are compared with 57 observational  $H(z)$  data points from DA and BAO methods.

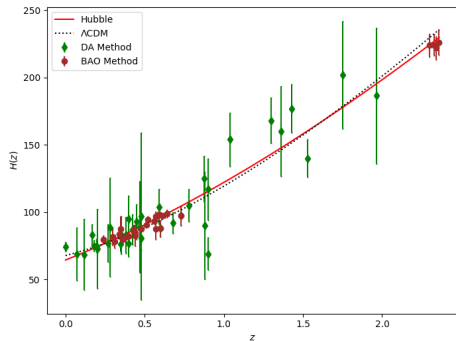


figure: Best-fit curve of  $H(z)$  vs redshift. Red: model; green diamonds: DA; red circles: BAO.

- Best-fit values:

- $\alpha = 0.542^{+0.019}_{-0.022}$
- $\beta = 52.9^{+2.3}_{-2.7}$
- $c_1 = -0.877^{+0.055}_{-0.058}$
- $H_0 = 64.39^{+0.04}_{-0.47}$  km/s/Mpc

- Model accuracy:

- $R^2 = 0.9321$
- RMSE = 11.0716

- $\Lambda$ CDM comparison:

$$H(z) = H_0 \sqrt{\Omega_{m0}(1+z)^3 + \Omega_{\Lambda 0}}$$

where  $H_0 = 67.8$ ,  $\Omega_{m0} = 0.3$ ,  
 $\Omega_{\Lambda 0} = 0.7$ .

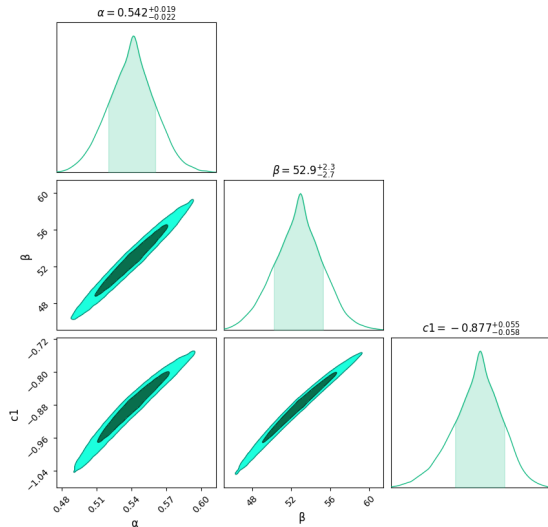


Figure: Confidence contours for  $\alpha$ ,  $\beta$ , and  $c_1$  at  $1\sigma$  and  $2\sigma$

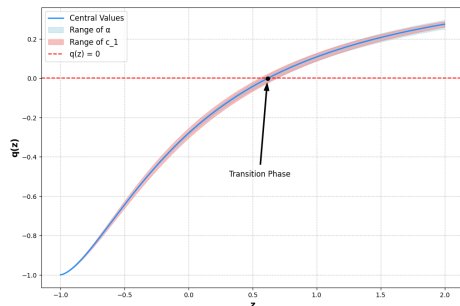
# Deceleration Parameter in Redshift

- From the scale factor–redshift relation, the deceleration parameter is expressed as:

$$q(z) = \alpha - \frac{\alpha + 1}{1 - c_1(1 + z)^{\alpha+1}}$$

- This function describes the evolution of the expansion rate — identifying transitions between deceleration and acceleration.
- The parameters used are:

$$\alpha = 0.542, \quad c_1 = -0.877, \quad H_0 = 64.39 \text{ km/s/Mpc}$$



figurePlot of  $q(z)$  vs redshift  $z$ .

# Deceleration Parameter in Redshift

- The plot of  $q(z)$  shows that at low redshift ( $z \approx -1$ ),  $q \approx -1$ , indicating an accelerating phase.
- As  $z$  increases,  $q(z)$  transitions to positive values, indicating a decelerating phase in the early universe.
- The red dashed line at  $q = 0$  marks the boundary between acceleration and deceleration.
- The black dot marks the transition point around  $z \approx 0.5$ .
- Shaded regions:
  - Blue: uncertainty due to  $\alpha$
  - Red: uncertainty due to  $c_1$
- The model yields:

$$R^2 = 0.9321, \quad \text{RMSE} = 11.0716$$

showing strong agreement with observational data and robustness of parameter constraints.

# Energy Density as a Function of Redshift

- The energy density  $\rho(z)$  is derived as:

$$\rho(z) = \left\{ \frac{9\beta^2 [(1+z)^{-(\alpha+1)} - c_1]^2}{(2+n)^2(1-2\xi)(\alpha+1)^2} (1+2n)(1+z) \right\}$$

- This describes how energy density evolves with redshift based on model parameters.

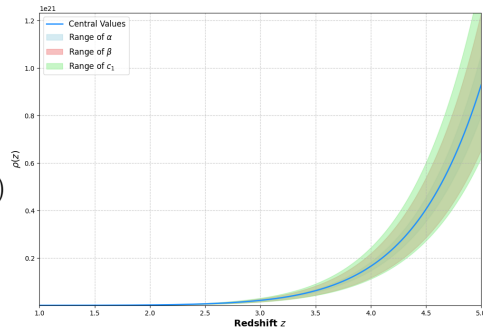


figure Energy density  $\rho(z)$  vs redshift.

# Energy Density as a Function of Redshift

- The plot of energy density illustrates how  $\rho(z)$  increases rapidly as redshift increases, consistent with a denser early universe.
- The blue curve shows the best-fit density evolution; shaded regions indicate uncertainty:
  - Blue shaded: uncertainty from  $\alpha$
  - Red shaded: uncertainty from  $\beta$
  - Green shaded: uncertainty from  $c_1$
- The growth in  $\rho(z)$  is highly sensitive to  $c_1$ , especially at high  $z$ , which corresponds to early universe epochs.
- This behavior supports the standard picture of structure formation, where the universe was more compact and energetic at earlier times.
- The expression fits well with observational trends and reflects early-universe matter dominance.



# Pressure as a Function of Redshift

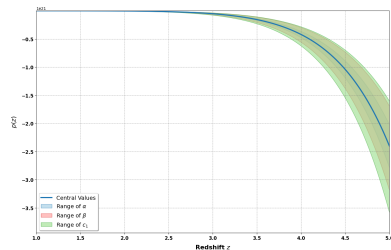
- The pressure  $p(z)$  is given by the expression:

$$p(z) = \frac{1}{\xi} \left\{ \frac{9\beta^2 [(1+z)^{-(\alpha+1)} - c_1]^2}{(2+n)^2(1-2\xi)(\alpha+1)^2} (1+2n)(1+z)^{2(\alpha+1)} - \frac{\zeta}{1-2\xi} \right\}^{\frac{1-\xi}{\xi}}$$

$$\times \left\{ \frac{6\beta^2 [(1+z)^{-(\alpha+1)} - c_1]}{(2+n)(\alpha+1)} (1+z)^{\alpha+1} \right.$$

$$+ [9 - 2(\alpha+1)(2+n)] \frac{3\beta^2 [(1+z)^{-(\alpha+1)} - c_1]^2}{(2+n)^2(\alpha+1)^2} (1+z)^{2(\alpha+1)}$$

$$\left. - \zeta - (1-\xi) \left[ \frac{9\beta^2 [(1+z)^{-(\alpha+1)} - c_1]^2}{(2+n)^2(1-2\xi)(\alpha+1)^2} (1+2n)(1+z)^{2(\alpha+1)} - \frac{\zeta}{1-2\xi} \right] \right\}$$



Pressure  $p(z)$  vs redshift.

# Pressure as a Function of Redshift

- The above Figure shows the behavior of pressure  $p(z)$  across redshift  $z$ .
- At higher redshifts, pressure becomes more negative — indicating dark energy dominance.
- The green-shaded region dominates at high  $z$ , highlighting the strong sensitivity of pressure to  $c_1$  during early cosmic times.
- This behavior aligns well with the theoretical expectation of negative pressure driving accelerated expansion in the late universe.

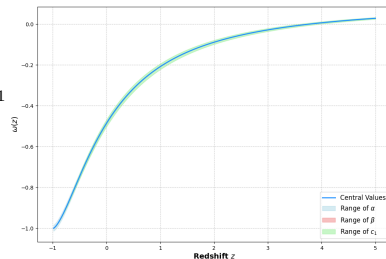
# Equation of State Parameter $\omega(z)$

- The equation of state (EoS) parameter  $\omega(z)$  is:

$$\omega(z) = -1 + \xi + \frac{1}{\xi} \left\{ \frac{9\beta^2 [(1+z)^{-(\alpha+1)} - c_1]^2}{(2+n)^2(1-2\xi)(\alpha+1)^2} (1+2n)(1+z)^{2(\alpha+1)} - \frac{\zeta}{1-2\xi} \right\}^{-1}$$

$$\times \left\{ \frac{6\beta^2 [(1+z)^{-(\alpha+1)} - c_1]}{(2+n)(\alpha+1)} (1+z)^{\alpha+1} + [9 - 2(\alpha+1)(2+n)] \right.$$

$$\times \left. \frac{3\beta^2 [(1+z)^{-(\alpha+1)} - c_1]^2}{(2+n)^2(\alpha+1)^2} (1+z)^{2(\alpha+1)} - \zeta \right\}$$



parameter  $\omega(z)$  vs redshift.

# Equation of State Parameter $\omega(z)$

- Figure 19 illustrates the evolution of the EoS parameter  $\omega(z)$  with redshift  $z$ .
- The shaded regions indicate uncertainties due to:
  - Light blue: variation in  $\alpha$
  - Pink: variation in  $\beta$
  - Green: variation in  $c_1$
- At low redshift ( $z \approx 0$ ),  $\omega \approx -1$ , consistent with dark energy behavior.
- As  $z$  increases,  $\omega(z)$  rises gradually, indicating a transition toward matter-dominated conditions.
- The narrow shaded bands reflect stable model predictions with well-constrained parameters.

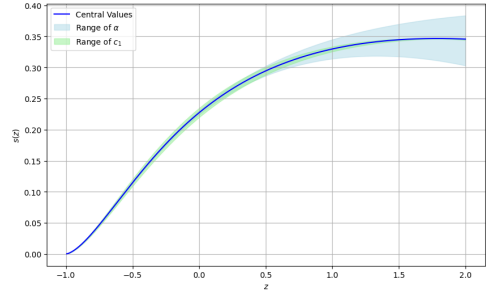
# Statefinder Diagnostic : The Parameter $s(z)$

- The statefinder parameters are defined as:

$$r = \frac{\ddot{a}}{aH^3}, \quad s = \frac{r - 1}{3\left(q - \frac{1}{2}\right)}$$

- The expression for  $s(z)$  is:

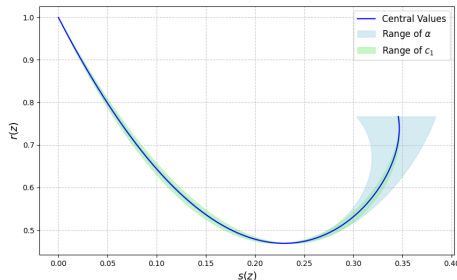
$$s(z) = \frac{2}{-3(3 + (2\alpha - 1)c_1(1+z)^{\alpha+1})(1 - c_1(1+z)^{\alpha+1})^2} \times \left\{ (1+z)^{\alpha+1}(\alpha+1)^2 \left( (1+z)^{-(\alpha+1)} - c_1 \right) - 3\alpha(\alpha+1) \left( (1+z)^{-(\alpha+1)} - c_1 \right)^2 (1+z)^{2\alpha+2} + \alpha(2\alpha+1) \left( (1+z)^{-(\alpha+1)} - c_1 \right)^3 (1+z)^{3\alpha+3} - (1 - c_1(1+z)^{\alpha+1})^3 \right\}$$



figurePlot of  $s(z)$  vs redshift  $z$ .

# Comparison of $r$ and $s$

- The statefinder pair  $(r, s)$  helps distinguish between various dark energy models.
- The point  $(r, s) = (1, 0)$  corresponds to the standard  $\Lambda$ CDM model.
- The region where  $r < 1$  and  $s > 0$  corresponds to the Quintessence model.



figurePlot of  $r(z)$  vs  $s(z)$

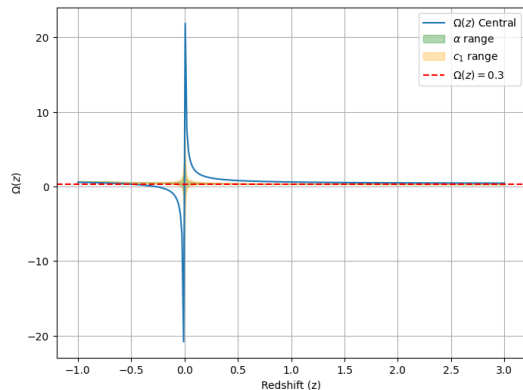
# Om Diagnostics

- The Om diagnostic helps distinguish dark energy models via expansion rate.
- Defined as:

$$\Omega(z) = \frac{\left(\frac{H(z)}{H_0}\right)^2 - 1}{(1+z)^3 - 1}$$

- Calculated Om diagnostics:

$$\Omega(z) = \frac{2c_1 [1 - (1+z)^{\alpha+1}] + c_1^2 [(1+z)^{\alpha+1} - 1]}{(1 - c_1)^2 ((1+z)^3 - 1)}$$



figurePlot of  $\Omega(z)$  vs redshift  $z$ .

# Discussion and Conclusion

- A LRS Bianchi Type-I cosmological model with perfect fluid was investigated in the  $f(R, \mathcal{L}_m)$  gravity framework.
- Exact field equations were derived and cosmological parameters like energy density, pressure, equation of state (EoS), Hubble parameter, deceleration parameter, expansion scalar, and shear scalar were evaluated.
- The Hubble parameter  $H(z)$  was fitted to 57 observational data points with an  $R^2 = 0.9321$ , showing strong agreement with the OHD data.
- Best-fit parameters:
  - $\alpha = 0.542^{+0.019}_{-0.022}$ ,  $\beta = 52.9^{+2.3}_{-2.7}$
  - $c_1 = -0.877^{+0.055}_{-0.058}$ ,  $H_0 = 64.39^{+0.04}_{-0.47}$  km/s/Mpc
- The model's predictions are consistent with the standard  $\Lambda$ CDM model, particularly at low redshifts.
- The deceleration parameter  $q(z)$  shows a transition from deceleration to acceleration near  $z \approx 0.5$ , supported by confidence regions in  $\alpha$  and  $c_1$ .



# Discussion and Conclusion

- Evolution of physical parameters:
  - $\rho(z)$ : Increases with redshift – denser early universe.
  - $p(z)$ : Transitions to negative values – consistent with dark energy.
  - $\omega(z)$ : Evolves from  $-1$  (dark energy) toward  $0$  – indicating Quintessence phase.
- Statefinder diagnostic:
  - The pair  $(r, s) = (1, 0)$  confirms  $\Lambda$ CDM consistency.
  - For best-fit values, model indicates Quintessence-like behavior for  $r < 1$ ,  $s > 0$ .
- Om diagnostic:
  - $\Omega(z)$  closely matches  $\Lambda$ CDM at higher  $z$ .
  - Deviations near  $z = 0$  suggest rapid late-time expansion.
- Overall, the model agrees with current cosmological observations and provides a viable alternative to  $\Lambda$ CDM within modified gravity frameworks.

# Thank You!

